Langmuir

LETTER

pubs.acs.org/Langmuir

Manipulation of Molecular Transport into Mesoporous Silica Thin Films by the Infiltration of Polyelectrolytes

Annette Brunsen,[†] Alejandra Calvo,[†] Federico J. Williams,[‡] Galo J. A. A. Soler-Illia,*[,†] and Omar Azzaroni*[,§]

[†]Gerencia de Química, Comisión Nacional de Energía Atómica (CNEA), Argentina

[‡]INQUIMAE, Facultad de Ciencias Exactas y Naturales, Universidad de Buenos Aires, Argentina

[§]Instituto de Investigaciones Fisicoquímicas Teóricas y Aplicadas (INIFTA), Departamento de Química, Facultad de Ciencias Exactas, Universidad Nacional de La Plata, CONICET, Argentina

Supporting Information

ABSTRACT: The design of hybrid mesoporous materials incorporating polymeric assemblies as versatile functional units has become a very fertile research area offering major opportunities for controlling molecular transport through interfaces. However, the creation of such functional materials depends critically on our ability to assemble polymeric units in a predictable manner within mesopores with dimensions comparable to the size of the macromolecular blocks themselves. In this work, we describe for the first time the manipulation of the molecular transport properties of mesoporous silica thin films by the direct infiltration of polyelectrolytes into the inner environment of the 3D porous framework. The hybrid architectures were built up through the infiltration−electrostatic assembly of polyallylamine (PAH) on the mesopore silica walls, and the resulting systems were studied by a combination of experimental techniques including ellipsoporosimetry, cyclic voltammetry and X-ray photoelectron spectroscopy, among others. Our results show that the infiltration−assembly of PAH alters the intrinsic cation-permselective properties of mesoporous silica films, rendering them ion-permeable mesochannels and enabling the unrestricted diffusion of cationic and anionic species through the hybrid interfacial architecture. Contrary to what happens during the electrostatic assembly of PAH on planar silica films (quantitative charge reversal), the surface charge of the mesoporous walls is completely neutralized upon assembling the cationic PAH layer (i.e., no charge reversal occurs). We consider this work to have profound implications not only on the molecular design of multifunctional mesoporous thin films but also on understanding the predominant role of nanoconfinement effects in dictating the functional properties of polymer−inorganic hybrid nanomaterials.

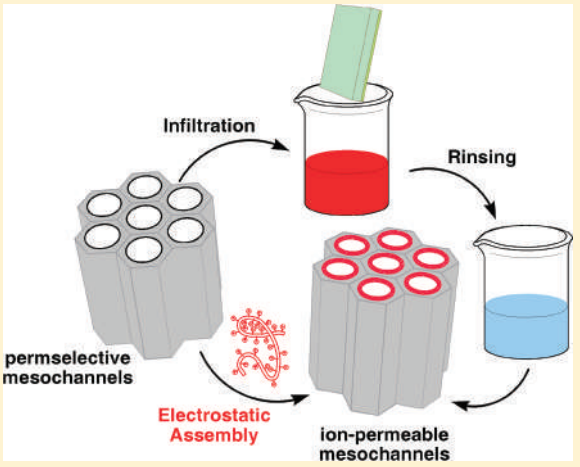

The rational design of robust platforms, permitting control and switching molecular transport, are of great interest in advanced applications such as drug delivery,[1] sensing,[2] glass nanoporous electrodes,[3] and membranes in batteries.[4] The generation of interfaces discriminating the transport of ionic species by charge is a mechanism that is well known in nature. Cell functions are based on active and passive transport phenomena through cell membranes. However, the manipulation of molecular transport in synthetic materials is not trivial because it demands control over a variety of physical phenomena down to the nanoscale. It is well known that the magnitude and polarity of the surface charges in the inner environment of the nanoscale pores are the main factors responsible for controlling the molecular transport of ionic species.[5−8] In this regard, extensive work on mesoporous inorganic thin films[9−11] has shown that this class of materials displays a unique set of functional features that make them the most suitable candidates for achieving this goal.[12−14] An alternative strategy could be the replication of biological membranes and the inclusion of biological pores inside them.[15] However, the advantageous aspects of inorganic and organic−inorganic hybrid systems can be seen in their robustness and substrate tolerance and the tunability of the interfacial architecture such as the thickness, pore size, and numerous modification strategies. To date, the modification of transport properties of mesoporous films has been carried out almost exclusively by adding functional organic groups[13] or postgrafting polymers to the mesoporous surface.[9b,14] In this work, we show the facile preparation of robust polymer−mesoporous hybrid materials displaying controllable transport properties by the simple electrostatic assembly of polyelectrolytes into

Received: February 7, 2011
Revised: March 15, 2011
Published: March 22, 2011

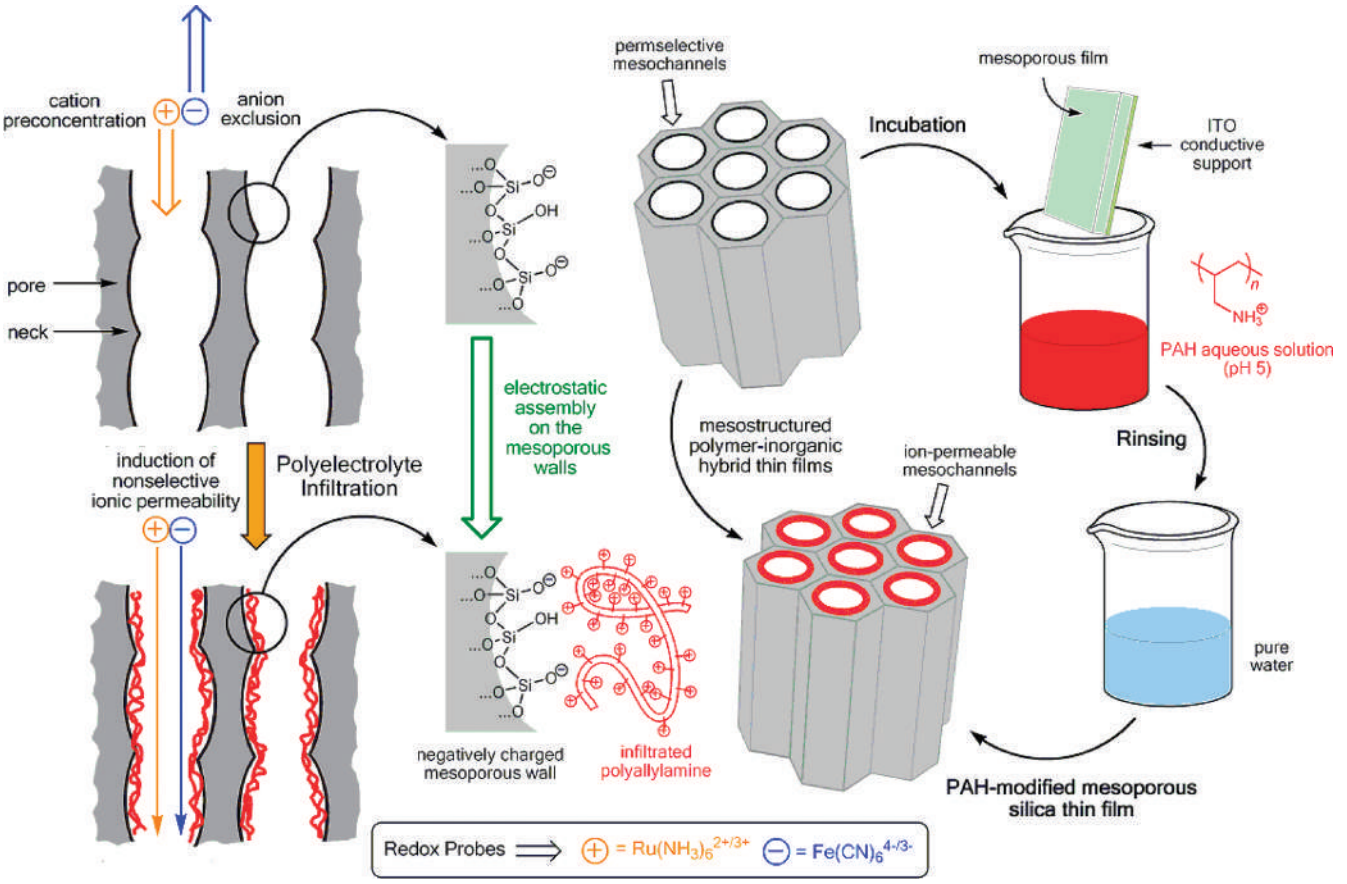

Figure 1. Schematic depiction of the infiltration of polyallylamine (PAH) inside the mesoporous silica film leading to the electrostatic assembly of the polyelectrolyte on the inner mesoporous walls.

mesoporous silica thin films. This strategy enabled us to manipulate/reverse the permselectivity properties of mesoporous silica thin films, thus opening a platform for easily tuning chemical properties in confined environments and investigating electrostatic interactions on the nanoscale.

Mesoporous silica films were obtained via one-pot sol−gel synthesis and dip coating onto silica and indium tin oxide (ITO) substrates using a sol containing tetraethoxysilane as the oxide precursor and nonionic block-copolymer template Pluronic-F127 (details in Supporting Information). This experimental protocol adapted from ref 16 led to 170-nm-thick mesoporous silica films presenting large, easily accessible mesopores with a pore diameter of approximately 10 nm as indicated by field effect scanning electron microscopy (FE-SEM) (details in Supporting Information). The presence of acid silanol groups at the silica walls and the resulting pH-dependent charge led to the development of negative surface charges on silica at pH >2. This leads, in general, to permselective properties of the mesoporous architecture, allowing selective transport or the exclusion of ions. To manipulate the permselective and the chemical properties in an easy and straightforward manner, we electrostatically assembled poly(allylamine) (PAH, $M_w \approx 15$ KDa) onto the silica mesopore walls. The infiltration of polyelectrolytes into mesoporous silica has been formerly explored by Caruso and collaborators[17a,b] and subsequently exploited to build up nanoporous polymer-based spheres for delivery purposes.[17c,d] They studied the infiltration of poly(acrylic acid) (PAA) of different molecular weights in amine-functionalized mesoporous silica particles with different pore sizes and found that electrostatic interactions between the polyelectrolyte and the pore walls dominate the infiltration process to a great extent. Along these lines, PAH infiltration was accomplished by simply incubating the mesoporous silica films in an aqueous solution of the commercially available polyelectrolyte at pH 5 to ensure opposite charges on the mesoporous film walls and PAH (Figure 1). This experimental protocol is analogous to the one typically used for LBL deposition in aqueous media.[18]

The presence of polyallylamine in the mesoporous samples was monitored by diffuse reflectance infrared Fourier transform spectroscopy (DRIFTS, data not shown) and then corroborated by X-ray photoelectron spectroscopy (XPS, Figure 2). At this point, it is worth mentioning that under our experimental conditions XPS probes the film surface (including pore openings and film walls) up to a penetration depth of ∼9 nm, corresponding to nearly two pore layers or ∼5% of the entire film thickness.[13f] Figure 2 shows the XPS results for the mesoporous silica films (blue trace). The spectra clearly show the presence of the Si 2p signal at 104.9 eV and the absence of the N 1s signal at 400.1 eV. Conversely, the XPS spectrum of the incubated films (Figure 2, red trace) revealed the appearance of the N 1s signal for the PAH-infiltrated mesoporous films. From the XPS characterization, we estimated the N/Si ratio to be 1:75.

Results consistent with polymer incorporation within the pores were obtained by spectroscopic ellipsometry. Ellipsometric data of mesoporous films prior to and after incubation with polyallylamine were satisfactorily adjusted with a single mesoporous

dx.doi.org/10.1021/la200501h |*Langmuir* 2011, 27, 4328–4333

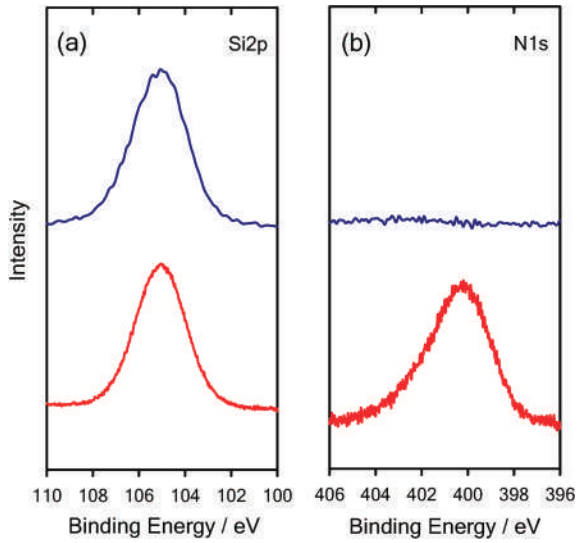

Figure 2. XP spectra of a bare mesoporous silica film (blue trace) and a PAH-modified silica film (red trace) in the binding-energy regions corresponding to (a) Si 2p and (b) N 1s.

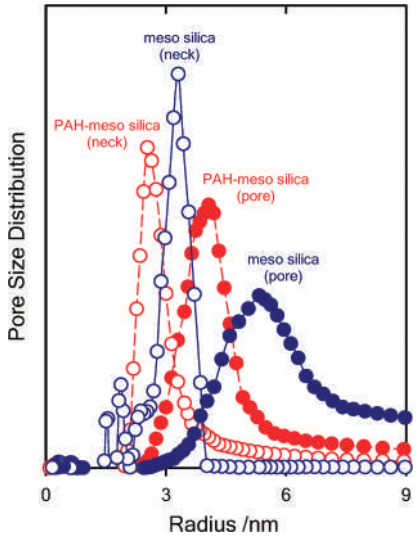

Figure 3. Pore size distribution of bare mesoporous silica (pore, blue ●; neck, blue ○) and PAH-infiltrated mesoporous silica films (pore, red ●; neck, red ○) as determined by ellipso-porosimetry.

layer model, leading to the assumption that the polymer is evenly distributed throughout the entire film, not only at the film surface. Therefore, we can assume that the polymer loading obtained from XPS is representative of the global film composition. Additionally, ellipso-porosimetry[19] was performed to study the effect of poly(allylamine) on the pore size distribution of the mesoporous films. A 5% reduction in the free pore volume was observed upon inclusion of the polymer (details in Supporting Information). The pore and interpore neck size distributions before and after incubation with polyallylamine were extracted from the adsorption and desorption curves, respectively.[20] Figure 3 shows that pore and neck diameters are reduced from 5.3 and 3.3 nm to 4.1 and 2.6 nm, respectively, upon the mesoporous structure being infiltrated by the polyeletrolyte.

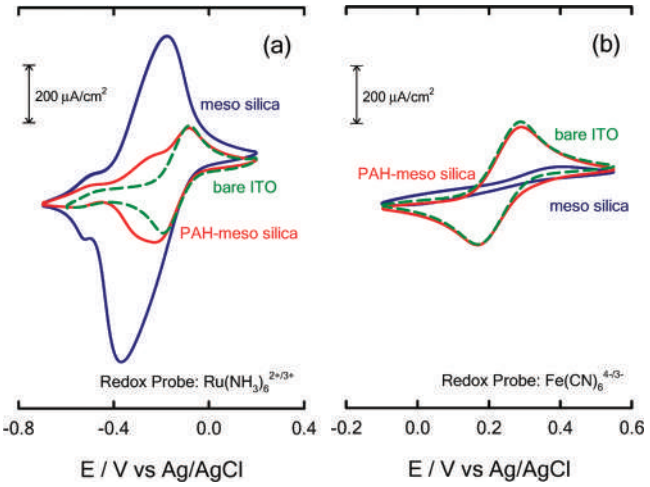

Figure 4. Cyclic voltammetric studies of molecular transport through mesoporous thin films using (a) $Ru(NH_3)_6^{3+}$ as a cationic redox probe and (b) $Fe(CN)_6^{3-}$ as an anionic redox probe. The different traces correspond to (blue trace) a bare mesoporous silica film, (red trace) a PAH-infiltrated mesoporous silica film, and (dashed green trace) a bare ITO substrate. Scan rate: 200 mV/s. Electrolyte: 1 mM redox probe + 0.1 M KCl (pH 5).

The narrowing of 1.2 nm in the pore diameter and 0.7 nm in the neck dimension most probably corresponds to one layer of PAH. It is well known from previous reports that one PAH layer results in a thickness increase of 0.6−1 nm.[21]

Having corroborated the surface functionalization of the pore walls, the influence of the functionalization on the molecular transport properties was studied by cyclic voltammetry.[22] To investigate the permselectivity, the diffusion of charged species through mesoporous films supported on ITO was electrochemically probed using anionic and cationic electroactive probes $Fe(CN_6)^{3-}$ and $Ru(NH_3)_6^{3+}$. Figure 4 comparatively displays the cyclic voltammograms of bare (blue trace) and PAH-modified (red trace) ITO-supported mesoporous silica thin films in the presence of 1 mM $Fe(CN_6)^{3-}$ and $Ru(NH_3)_6^{3+}$ at pH 5 by employing 0.1 M KCl as the supporting electrolyte. In the case of bare mesoporous silica films, a well-defined electrochemical response of $Ru(NH_3)_6^{3+}$ ions was observed whereas similar experiments performed in the presence of $Fe(CN_6)^{3-}$ revealed that the electron transfer at the underlying ITO interface was strongly hindered. This can be ascribed to the fact that the negatively charged pore walls exclude the anionic probes from the inner surroundings of the inorganic film. In a similar vein, the enhanced electrochemical response, as compared to the cyclic voltammogram of the bare ITO electrode in the presence of the redox probe solution (Figure 4, dashed green trace), reflects the fact that the silica mesoporous film is able to preconcentrate $Ru(NH_3)_6^{3+}$ species in the inner environment of the 3D pore array. In this scenario, the attractive electrostatic interactions in the mesopore environment are the main driving force leading to the preconcentration of the cationic probe within the porous framework.

However, repeating the same electrochemical experiments in PAH-modified mesoporous films revealed important changes in the transport properties of the interfacial architecture. The electrochemical signal corresponding to $Ru(NH_3)_6^{3+}$ decreased but it was still detectable without evidence of electron-transfer hindrance. Interestingly, we observed that the magnitude of the

dx.doi.org/10.1021/la200501h |*Langmuir* 2011, 27, 4328–4333

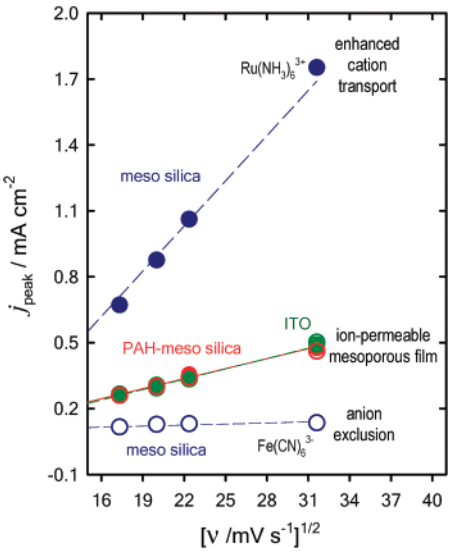

Figure 5. Representation of the peak current densities (j_{peak}) as a function of the square root of the scan rate ($\nu^{1/2}$). The different symbols correspond to (i) $Ru(NH_3)_6^{3+}$ cations probing (blue ●) bare mesoporous silica films, (red ●) PAH-infiltrated mesoporous silica films, and (green ●) bare ITO electrodes and (ii) $Fe(CN_6)^{3-}$ anions probing (blue ○) bare mesoporous silica films, (red ○) PAH-infiltrated mesoporous silica films, and (green ○) bare ITO electrodes. Electrolyte: 1 mM redox probe + 0.1 M KCl (pH 5).

detected electrochemical signal is comparable to that measured on bare ITO electrodes. Changes in the voltammetric response of mesoporous electrodes reflect the changes in probe concentration or diffusion due to the architecture or electrostatic environment of the pores. This indicates that (i) the redox process is feasible, (ii) there are no significant preconcentration effects, (iii) no significant exclusion of cationic species takes place, and (iv) the concentration of $Ru(NH_3)_6^{3+}$ species close to the ITO underlayer in PAH-modified films is comparable to that detected in bare ITO electrodes. To corroborate the diffusional nature of the detected electrochemical signal, we repeated cyclic voltammograms at different potential scan rates (Figure 5). The well-defined dependence of the peak current density (j_{peak}) on $\nu^{1/2}$, with ν being the potential scan rate, further supports the idea that the electron-transfer processes is coupled to the diffusion of the redox probe to the underlying ITO surface. Figure 5 describes the j_{peak} versus $\nu^{1/2}$ plot for the different interfacial architectures in the presence of $Ru(NH_3)_6^{3+}$. This plot reveals two interesting features. First, the enhanced voltammetric response of $Ru(NH_3)_6^{3+}$ in mesoporous silica is even more pronounced at high scan rates. A higher slope indicates that the molecular transport of the cationic probe is facilitated in comparison to that of PAH-modified films provided that the voltammetric peaks are proportional to $D^{1/2}C$ (with D being the effective diffusion coefficient and C being the concentration of the probe diffusing in the mesoporous film).[23] Then, the j_{peak} versus $\nu^{1/2}$ plot for PAH-modified films is identical to that obtained from similar experiments on bare ITO substrates. This strongly suggests that the molecular transport of $Ru(NH_3)_6^{3+}$ ions through the PAH-infiltrated mesoporous films involves free diffusion of the species from solution and is not governed by strong interactions with the pore walls.

Changes in the transport properties of PAH-modified films were also evident when probed with $Fe(CN_6)^{3-}$ species. In stark contrast to that observed in bare mesoporous films, the transport of $Fe(CN_6)^{3-}$ anions through the PAH-infiltrated porous substrate proceeded with no hindrance and in accordance with a freely diffusing species approaching the ITO surface. A direct comparison of results from PAH-infiltrated mesoporous films and bare ITO revealed that the magnitude of the voltammetric signals and the dependence of j_{peak} on $\nu^{1/2}$ are similar,[24] thus suggesting that the diffusion of $Fe(CN_6)^{3-}$ into the mesoporous film is governed neither by repulsive electrostatic interactions leading to ion exclusion nor by attractive electrostatic interactions promoting the preconcentration of the redox probe. Furthermore, these results corroborate the idea that the polyelectrolyte is evenly distributed within the film; otherwise, the presence of negatively charged silica close to the ITO interface would repel the anionic $Fe(CN_6)^{3-}$ species from the electrode surface, which is not observed.

Within this framework, we can conclude that the presence of PAH in the inner environment of the mesopores promotes the neutralization of the silanol groups that are responsible for the preconcentration of $Ru(NH_3)_6^{3+}$ cations and the exclusion of $Fe(CN_6)^{3-}$ anions. Notably, the absence of $Ru(NH_3)_6^{3+}$ exclusion and the detection of electrochemical signals that are comparable to those measured on bare ITO support the idea that no charge reversal is taking place upon polyelectrolyte assembly on the mesoporous walls. Otherwise, the appearance of net positive charges on the mesoporous walls would have triggered cation-permselective properties in the interfacial assembly as well as the enhanced voltammetric response of the $Fe(CN_6)^{3-}$ ions. In the case of electrostatic assembly, the strong confinement dictates how far the polyelectrolyte loops and tails dangle into the pore, thus determining the extent of charge reversal.[25] For instance, spatially confined species experience enhanced intermolecular interaction, which results in highly cooperative phenomena. In a physically confined environment, structural frustration[26] and confinement-induced entropy loss[27,28] can play dominant roles in determining the molecular organization, which in turn governs the physical chemistry of any polymeric system when it is confined in spaces comparable to its molecular dimensions. For example, the physical nanoconfinement of polyelectrolytes can trigger the irreversible formation of ion pairs.[29] Recent noteworthy work by Savariar et al. indicates that typical charge reversal on planar electrostatic assemblies is no longer applicable within a nanopore.[30] Upon assembling polypropyleneimine (PPI) dendrimers (second generation, G2) on poly(acrylic acid) (PAA)-modified nanopores, the diameter was reduced from 28 to 23 nm. Because positively charged PPI dendrimers decorated the pore walls, it was expected that anionic probe calcein would diffuse through the pores more rapidly than would cationic rhodamine 6G. Control experiments revealed no observable differences in the diffusion rates of both probes, but more importantly, no differences were observed after comparing the diffusion of both dyes through PPI-G2/PAA-modified and unfunctionalized (uncharged) pores. This suggests that PPI-G2 dendrimers have essentially neutralized the negative charge of PAA; however, they were not able to provide the pore walls with an overall positive charge (i.e., no charge reversal). In close resemblance to Savariar's work, our experimental results indicate that the electrostatic assembly of PAH into the mesopores removes the typical ion-selective gating properties of bare or organically modified mesoporous silica films. (See refs 13c and 14.)

dx.doi.org/10.1021/la200501h |*Langmuir* 2011, 27, 4328–4333

The infiltration of the polycation transforms the original inorganic film into an ion-permeable mesostructured interfacial architecture in which cations and anions can freely diffuse into its inner environment.

In summary, we showed for the first time the use of infiltrated polyelectrolytes as versatile building blocks enabling the manipulation of the molecular transport characteristics of mesoporous silica films by simple postsynthetic experimental protocols. Considering the simplicity of this process and the widely available palette of polymers and mesoporous systems, this concept can be easily extended to a variety of polyelectrolytes, mesoporous materials, and chemical functionalities.[31] For example, our results demonstrating the construction of robust mesoporous silica films permitting the unrestricted or unbiased diffusion of cations and anions can be very useful in preconditioning mesotemplates[32] prior to the impregnation of ionic precursor species. This versatile route toward polymer-modified mesoporous films opens a path not only to a new type of highly functional interfacial architectures but also to the study of the diffusion of polyelectrolytes in nanoconfinement, independently of the surface charge development.

■ ASSOCIATED CONTENT

Supporting Information. Experimental protocols, field-effect scanning electron microscopy, ellipso-porosimetry, X-ray photoelectron spectroscopy, and electrochemical characterization. This material is available free of charge via the Internet at http://pubs.acs.org.

■ AUTHOR INFORMATION

Corresponding Author

*(G.J.A.A.S.-I.) E-mail: gsoler@cnea.gov.ar. Homepage: http://www.qi.fcen.uba.ar/personales/soler-illia.htm. (O.A.) E-mail: azzaroni@inifta.unlp.edu.ar. Homepage: http://softmatter.quimica.unlp.edu.ar.

■ ACKNOWLEDGMENT

We gratefully acknowledge financial support from Agencia Nacional de Promoción Científica y Tecnológica (ANPCyT) (PICT 34518 and 1848, PAE 2004 22711, and PICT-PRH 163/08), Centro Interdisciplinario de Nanociencia y Nanotecnología (CINN, PAE 2006 37063, projects PRH 2007-74-PIDRI no. 74 and PME 00038), Fundación Petruzza, Gabbos (DG-017), Max-Planck-Gesellschaft (MPG), Consejo Nacional de Investigaciones Científicas y Técnicas (CONICET), Alexander von Humbolt Stiftung, and Laboratório Nacional de Luz Síncrotron (LNLS). A.C. acknowledges CONICET and Tenaris for a scholarship. F.J.W., G.J.A.A.S.-I., and O.A are staff members of CONICET.

■ REFERENCES

(1) Cauda, V.; Muhlstein, L.; Onida, B.; Bein, T. *Microporous Mesoporous Mater.* **2009**, *118*, 435.

(2) Melde, B. J.; Johnson, B. J.; Charles, P. T. *Sensors* **2008**, *8*, 5202.

(3) Wang, G. L.; Zhang, B.; Wayment, J. R.; Harris, J. M.; White, H. S. *J. Am. Chem. Soc.* **2006**, *128*, 7679.

(4) Wang, C.; Wang, D.; Wang, Q.; Wang, L. *Electrochim. Acta* **2010**, *55*, 6420.

(5) (a) Kuo, T.-C.; Sloan, L. A.; Sweedler, J. V.; Bohn, P. W. *Langmuir* **2001**, *17*, 6298. (b) Boissiere, C.; Martines, M. U.; Larbot, A.; Prouzet, E. *J. Membr. Sci.* **2005**, *251*, 17.

(6) (a) Yameen, B.; Ali, M.; Neumann, R.; Ensinger, W.; Knoll, W.; Azzaroni, O. *Chem. Commun.* **2010**, *46*, 1908. (b) Yameen, B.; Ali, M.; Neumann, R.; Ensinger, W.; Knoll, W.; Azzaroni, O. *J. Am. Chem. Soc.* **2009**, *131*, 2070.

(7) (a) Siwy, Z. S. *Adv. Funct. Mater.* **2006**, *16*, 735. (b) Bohn, P. W. *Annu. Rev. Anal. Chem.* **2009**, *2*, 279.

(8) (a) Tagliazucchi, M.; Azzaroni, O.; Szleifer, I. *J. Am. Chem. Soc.* **2010**, *132*, 12404. (b) Yameen, B.; Ali, M.; Neumann, R.; Ensinger, W.; Knoll, W.; Azzaroni, O. *Nano Lett.* **2009**, *9*, 2788.

(9) (a) Innocenzi, P.; Malfatti, L.; Kidchob, T.; Falcaro, P. *Chem. Mater.* **2009**, *21*, 2555. (b) Soler-Illia, G. J. A. A.; Azzaroni, O. *Chem Soc. Rev.* **2011**, *40*, 1107.

(10) Sanchez, C.; Shea, K. J.; Kitagawa, S. *Chem. Soc. Rev.* **2011**, *40*, 471 (Hybrid Materials themed issue).

(11) Lebeau, B.; Innocenzi, P. *Chem. Soc. Rev.* **2011**, *40*, 886–906.

(12) (a) Casasús, R.; Climent, E.; Marcos, M. D.; Martínez-Máñez, R.; Sancenón, F.; Soto, J.; Amorós, P.; Cano, J.; Ruiz, E. *J. Am. Chem. Soc.* **2008**, *130*, 1903. (b) Aznar, E.; Marcos, M. D.; Martínez-Máñez, R.; Sancenón, F.; Soto, J.; Amorós, P.; Guillem, C. *J. Am. Chem. Soc.* **2009**, *131*, 6833. (c) Coll, C.; Casasús, R.; Aznar, E.; Marcos, M. D.; Martínez-Máñez, R.; Sancenón, F.; Soto, J.; Amorós, P. *Chem. Commun.* **2007**, 1957.

(13) (a) Taffa, D. H.; Kathiresan, M.; Walder, L.; Seelandt, B.; Wark, M. *Phys. Chem. Chem. Phys.* **2010**, *12*, 1473. (b) Marschall, R.; Rathouský, J.; Wark, M. *Chem. Mater.* **2007**, *19*, 6401. (c) Fattakhova-Rohlfing, D.; Wark, M.; Rathouský, J. *Chem. Mater.* **2007**, *19*, 1640. (d) Etienne, M.; Quach, A.; Grosso, D.; Nicole, L.; Sanchez, C.; Walcarius, A. *Chem. Mater.* **2007**, *19*, 844. (e) Etienne, M.; Grosso, D.; Boissière, C.; Sanchez, C.; Walcarius, A. *Chem. Commun.* **2005**, 4566. (f) Calvo, A.; Angelome, P. C.; Sanchez, V. M.; Scherlis, D. A.; Williams, F. J.; Soler-Illia, G. *Chem. Mater.* **2008**, *20*, 4661.

(14) (a) Calvo, A.; Yameen, B.; Williams, F. J.; Azzaroni, O.; Soler-Illia, G. J. A. A. *Chem. Commun.* **2009**, 2553. (b) Calvo, A.; Yameen, B.; Williams, F. J.; Soler-Illia, G. J. A. A.; Azzaroni, O. *J. Am. Chem. Soc.* **2009**, *131*, 10866. (c) Fu, Q.; Rao, G. V. R.; Ward, T. L.; Lu, Y.; Lopez, G. P. *Langmuir* **2007**, *23*, 170. (d) Fu, Q.; Rao, G. V. R.; Ista, L. K.; Wu, Y.; Andrzejewski, B. P.; Sklar, L. A.; Ward, T. L.; Lopez, G. P. *Adv. Mater.* **2003**, *15*, 1262.

(15) (a) Sackmann, E. *Science* **1996**, *271*, 43. (b) Bally, M.; Bailey, K.; Sugihara, K.; Grieshaber, D.; Vörös, J.; Städler, B. *Small* **2010**, *6*, 2481.

(16) Bellino, M. G.; Regazzoni, A. E.; Soler-Illia, G. J. A. A. *ACS Appl. Mater. Interfaces* **2010**, *2*, 360.

(17) (a) Angelatos, A. S.; Wang, Y.; Caruso, F. *Langmuir* **2008**, *24*, 4224. (b) Wang, Y.; Angelatos, A. S.; Dunstan, D. E.; Caruso, F. *Macromolecules* **2007**, *40*, 7594. (c) Wang, Y.; Caruso, F. *Chem. Mater.* **2006**, *18*, 4089. (d) Wang, Y.; Bansal, V.; Zelikin, A. N.; Caruso, F. *Nano Lett.* **2008**, *8*, 1741.

(18) Decher, G. In *Multilayer Thin Films*; Decher, G., Schlenoff, J. B., Eds.; Wiley-VCH: Weinheim, Germany, 2002; Chapter 1, pp 1−46.

(19) Boissiere, C.; Grosso, D.; Lepoutre, S.; Nicole, L.; Brunet-Bruneau, A.; Sanchez, C. *Langmuir* **2005**, *21*, 12362.

(20) Kruk, M.; Jaroniec, M. *Chem. Mater.* **2003**, *15*, 2942.

(21) Lowack, K.; Helm, C. A. *Macromolecules* **1998**, *31*, 823.

(22) Crooks, R. M., Chailapakul, O.; Ross, C. B.; Sun, L.; Schoer, J. L. In *Interfacial Design and Chemical Sensing*; Mallouk, T. E., Harrison, D. J., Eds.; American Chemical Society: Washington, DC, 1994; Chapter 10, pp 104−122.

(23) Bard, A. J. *Integrated Chemical Systems: A Chemical Approach to Nanotechnology*; John Wiley & Sons: New York, 1994; Chapter 5, pp 184−226.

(24) For the sake of clarity, we have included an alternative comparative plot in the Supporting Information.

(25) Ali, M.; Yameen, B.; Cervera, J.; Ramírez, P.; Neumann, R.; Ensinger, W.; Knoll, W.; Azzaroni, O. *J. Am. Chem. Soc.* **2010**, *132*, 8338.

(26) Lambooy, P.; Russell, T. P.; Kellogg, G. J.; Mayes, A. M.; Gallagher, P. D.; Satija, S. K. *Phys. Rev. Lett.* **1994**, *72*, 28992.
(27) Wu, Y.; Cheng, G.; Katsov, K.; Sides, S. W.; Wang, J.; Tang, J.; Fredrickson, G. H.; Moskovits, M.; Stucky, G. D. *Nat. Mater.* **2004**, *3*, 816.
(28) Nguyen, T. Q.; Wu, J. J.; Doan, V.; Schwartz, B. J.; Tolbert, S. H. *Science* **2000**, *288*, 652.
(29) Azzaroni, O.; Trappmann, B.; van Rijn, P.; Zhou, F.; Kong, B.; Huck, W. T. S. *Angew. Chem., Int. Ed.* **2006**, *45*, 7440.
(30) Savariar, E. N.; Sochat, M. M.; Klaikherd, A.; Thayumanavan, S. *Angew. Chem., Int. Ed.* **2009**, *48*, 110.
(31) (a) Gómez-Romero, P.; Sanchez, C. *Functional Hybrid Materials*; Wiley-VCH: Weinheim, Germany, 2004; Chapter 1, pp 1−14. (b) Sanchez, C.; Soler-Illia, G. J. A. A.; Ribot, F.; Lalot, T.; Mayer, C. R.; Cabuil, V. *Chem. Mater.* **2001**, *13*, 30613.(c) Hoffmann, F.; Fröba, M. *The Supramolecular Chemistry of Organic-Inorganic Hybrid Materials*; Rurack, K., Martínez-Máñez, R., Eds.; Wiley: Chichester, U.K., 2010; Chapter 3, pp 39−111.
(32) Calvo, A.; Fuertes, M. C.; Yameen, B.; Williams, F. J.; Azzaroni, O.; Soler-Illia, G. J. A. A. *Langmuir* **2010**, *26*, 5559.